World Journal of

Gastroenterology

World Journal of Gastroenterology

Contents

Contents

Contents

ABOUT COVER

Editorial Board Member of *World Journal of Gastroenterology*, Dmitry S Bordin, MD, PhD, Chief Doctor, Professor, Department of Pancreatic, Biliary and Upper GI Tract Diseases, A.S. Loginov Moscow Clinical Scientific Center, Moscow 111123, Russia. dmitrybordin@gmail.com

AIMS AND SCOPE

The primary aim of *World Journal of Gastroenterology* (*WJG*, *World J Gastroenterol*) is to provide scholars and readers from various fields of gastroenterology and hepatology with a platform to publish high-quality basic and clinical research articles and communicate their research findings online. *WJG* mainly publishes articles reporting research results and findings obtained in the field of gastroenterology and hepatology and covering a wide range of topics including gastroenterology, hepatology, gastrointestinal endoscopy, gastrointestinal surgery, gastrointestinal oncology, and pediatric gastroenterology.

INDEXING/ABSTRACTING

The *WJG* is now abstracted and indexed in Science Citation Index Expanded (SCIE, also known as SciSearch®), Current Contents/Clinical Medicine, Journal Citation Reports, Index Medicus, MEDLINE, PubMed, PubMed Central, Scopus, Reference Citation Analysis, China National Knowledge Infrastructure, China Science and Technology Journal Database, and Superstar Journals Database. The 2022 edition of Journal Citation Reports® cites the 2021 impact factor (IF) for *WJG* as 5.374; IF without journal self cites: 5.187; 5-year IF: 5.715; Journal Citation Indicator: 0.84; Ranking: 31 among 93 journals in gastroenterology and hepatology; and Quartile category: Q2. The *WJG*'s CiteScore for 2021 is 8.1 and Scopus CiteScore rank 2021: Gastroenterology is 18/149.

RESPONSIBLE EDITORS FOR THIS ISSUE

Production Editor: *Yi-Xuan Cai*; **Production Department Director:** *Xiang Li*; **Editorial Office Director:** *Jia-Ru Fan*.

Role of advanced imaging techniques in the evaluation of oncological therapies in patients with colorectal liver metastases

Martina Caruso, Arnaldo Stanzione, Anna Prinster, Laura Micol Pizzuti, Arturo Brunetti, Simone Maurea, Pier Paolo Mainenti

Martina Caruso, Arnaldo Stanzione, Arturo Brunetti, Simone Maurea, Department of Advanced Biomedical Sciences, University of Naples "Federico II", Napoli 80131, Italy

Anna Prinster, Laura Micol Pizzuti, Pier Paolo Mainenti, Institute of Biostructures and Bioimaging, National Research Council, Napoli 80131, Italy

Corresponding author: Arnaldo Stanzione, MD, PhD, Postdoc, Department of Advanced Biomedical Sciences, University of Naples "Federico II", Via S. Pansini 5, Napoli 80131, Italy. arnaldo.stanzione@unina.it

Abstract

In patients with colorectal liver metastasis (CRLMs) unsuitable for surgery, oncological treatments, such as chemotherapy and targeted agents, can be performed. Cross-sectional imaging [computed tomography (CT), magnetic resonance imaging (MRI), 18-fluorodexoyglucose positron emission tomography with CT/MRI] evaluates the response of CRLMs to therapy, using post-treatment lesion shrinkage as a qualitative imaging parameter. This point is critical because the risk of toxicity induced by oncological treatments is not always balanced by an effective response to them. Consequently, there is a pressing need to define biomarkers that can predict treatment responses and estimate the likelihood of drug resistance in individual patients. Advanced quantitative imaging (diffusion-weighted imaging, perfusion imaging, molecular imaging) allows the *in vivo* evaluation of specific biological tissue features described as quantitative parameters. Furthermore, radiomics can represent large amounts of numerical and statistical information buried inside cross-sectional images as quantitative parameters. As a result, parametric analysis (PA) translates the numerical data contained in the voxels of each image into quantitative parameters representative of peculiar neoplastic features such as perfusion, structural heterogeneity, cellularity, oxygenation, and glucose consumption. PA could be a potentially useful imaging marker for predicting CRLMs treatment response. This review describes the role of PA applied to cross-sectional imaging in predicting the response to oncological therapies in patients with CRLMs.

Key Words: Colorectal cancer metastases; Prediction response; Computed tomography; Magnetic resonance imaging; Positron emission tomography; Parametric imaging

Core Tip: Chemotherapy and targeted agents can be administered to patients with colorectal liver metastasis (CRLM) unsuitable for surgery. The risk of toxicity requires identification of imaging biomarkers that can estimate the likelihood of response and drug resistance before starting therapy. Clinical validation may aid clinicians in tailoring their individual treatment regimens. In this setting, parametric analysis applied to cross-sectional imaging plays a crucial role in evaluating *in vivo* peculiar neoplastic features, such as perfusion, structural heterogeneity, cellularity, oxygenation, and glucose consumption. However, there is no consensus on the most promising imaging quantitative parameter to predict therapy response in CRLMs patients.

## INTRODUCTION

Colorectal cancer is one of the most common cancers worldwide and the fourth leading cause of cancer death[1]. Unfortunately, up to 19% of colorectal cancer patients present with liver metastasis at diagnosis, while up to 13% develop it within the 5-year follow-up[1]. Surgery plays a crucial role in improving the prognosis of colorectal liver metastasis (CRLMs), but only 20% of them are initially suitable for this approach[2]. Hence, systemic chemotherapy is the treatment of choice for the remaining 80% of patients with the aim of rendering metastases resectable and/or prolonging survival[3]. In clinical practice, systemic chemotherapy based on a combination of fluoropyrimidines with oxaliplatin and/or irinotecan is usually associated with targeted agents. The assessment of *KRAS*, *NRAS*, and *BRAF* genes status influences the choice of the most appropriate targeted agents: If they are wild-type, panitumumab or cetuximab, epidermal growth factor receptor (EGFR) antibodies, are preferred, whereas if they are mutated, bevacizumab, a vascular endothelial growth factor (VEGF) antibody, is chosen[4]. In this setting, the cross-sectional imaging evaluation, represented by computed tomography (CT), magnetic resonance imaging (MRI) and 2-[18F]fluoro-2-deoxy-D-glucose positron emission tomography (2-[18F]FDG-PET) associated with CT or MRI (2-[18F]FDG-PET/CT or MRI), is fundamental in the assessment of treatment response based on dimensional evaluation of tumour burden in consecutive scans through the application of standardised criteria, known as "Response Evaluation Criteria in Solid Tumours (RECIST, Figure 1)"[5-7]. These criteria have been very useful in the assessment of treatment response to cytotoxic chemotherapeutic agents, but the introduction of targeted agents with predominant cytostatic effects, such as anti-EGFR and anti-VEGF, makes them insufficient for adequate response imaging evaluation. Indeed, solid tumours may respond to these new agents by developing intra-tumoural necrotic areas and/or cystic, fibrotic, or myxoid degeneration, resulting in an overall increased, decreased, or unchanged size. Thus, the assessment of treatment response during follow-up based purely on dimensional evaluation of the tumour burden seems no longer sufficient. Furthermore, targeted agents are more expensive than cytotoxic agents and are burdened by hepatic toxicity (steatosis, hepatitis, sinusoidal obstruction syndrome, and impaired liver function). Considering these issues, identification of imaging biomarkers that can estimate the likelihood of response and drug resistance in individual patients before or immediately after starting therapy is mandatory. This critical point represents not only a clinician request to avoid unnecessary drug toxicity and the starting delay of alternative therapies, potentially more effective, but also an economic requirement to reduce futile health care costs.

The growth of neoplastic tissue is characterised by the activation of several biological processes, such as neoangiogenesis and anarchic cellular proliferation, which determine neoplastic heterogeneity for the coexistence of high cell density, necrotic, hypoxic, haemorrhagic, and necrotic areas. Neoplastic cells are characterised by increased metabolism and glucose consumption. Currently, these biological neoplastic processes as well as the neoplastic heterogeneity can be analysed *in vivo* applying several post-processing imaging analyses to different cross-sectional imaging techniques, such as diffusion-weighted imaging (DWI) on MRI, perfusion imaging on CT and MRI, and molecular imaging on 2-[18F]FDG-PET/CT and MRI. The *in vivo* structural, functional, and molecular information obtained from imaging is expressed through parametric parameters, which represent potentially useful biomarkers in clinical practice. Parametric analysis (PA) allows the extraction of numerical data contained in the voxels of each image and converts the extracted numerical data into quantitative parametric maps, which are
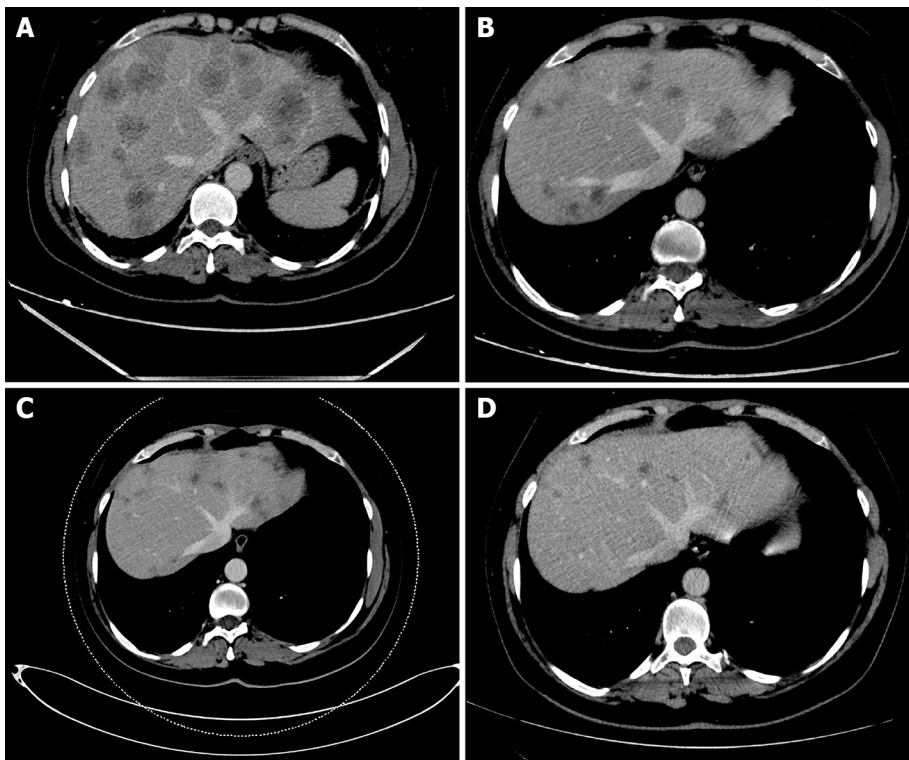
Figure 1 Contrast enhanced computed tomography images from a patient with colon cancer. A: Baseline computed tomography (CT) demonstrates the presence of multiple liver metastases; B: After four cycles of combined chemotherapy (folinic acid + fluorouracil + irinotecan + cetuximab) the CT scan shows a reduction in both size and number of liver metastases, which was classified as a partial response with Response Evaluation Criteria in Solid Tumours criteria; C and D: The partial response was then confirmed after (C) 8 and (D) 12 chemotherapy cycles.

representative of peculiar neoplastic features, such as perfusion, structural heterogeneity, cellularity, oxygenation, and glucose consumption, depending on the imaging modalities and techniques used. PA requires the drawing of a region of interest (ROI) or volume of interest that includes the target tissue for analysis. In recent years, PA has been enriched with radiomics, a complex multi-step process that allows the extraction of a huge amount of computational quantitative features from digital medical images, thereby increasing the potential role of cross-sectional imaging in the oncological field. Radiomics has recently emerged as a promising tool for discovering new imaging biomarkers by extracting and analysing numerous quantitative image features representative of tumour heterogeneity and phenotype. Radiomics combines quantitative imaging biomarkers with clinical reports and laboratory test values in statistical models[8].

Finally, the response to chemotherapeutic agents is influenced by their delivery to neoplastic tissues, which is influenced by the tumour microenvironment and cellular characteristics, such as uptake, retention, metabolic activation, and catabolism of drugs, as well as genetic factors such as DNA repair mechanisms[9]. The *in vivo* knowledge of peculiar neoplastic features through cross-sectional imaging may provide imaging biomarkers aiding in the prediction of treatment response and drug resistance. To date, several researchers have investigated the role of quantitative imaging parameters in the pre-treatment response prediction of CRLMs patients using MRI, CT, and 2-[18F]FDG-PET/CT or MRI[10, 11], but there is no clear consensus about which is the most promising imaging technique as well as the most promising quantitative imaging parameter. Therefore, this review aimed to describe the role of PA in predicting the response to oncological therapies in patients with CRLMs.

PA BASED ON MRI DIFFUSION TECHNIQUE

DWI with apparent diffusion coefficient maps

DWI is a functional MRI technique that measures the Brownian motion of water molecules in biological tissues, which is restricted by an increase in cellularity and architectural tissue changes[12]. Consequently, in tumour tissues, the dense cellularity associated with fibrosis, necrosis, neovascular-ization, and haemorrhages reduces the intercellular space, altering water diffusion properties and restricting Brownian motion. Diffusion-weighted MR images measure the apparent diffusion coefficient (ADC), which is inversely proportional to the cell density, presumably resulting from the tortuosity of

the interstitial space and the consequential limitation of water movement. Tumours with high cellularity tend to present low ADC values on diffusion-weighted MRI because of their high cellularity, characteristically presenting with restriction in these lesions. Therefore, using DWI, it is possible to obtain a parametric ADC map, which is composed of the ADC values calculated for each voxel and represents a quantitative measure of water molecule diffusion expressed as 10^{-3} mm^2/s. ADC is inversely related to tumour cellularity and is strongly affected by molecular viscosity, permeability of the membrane separating the intra- and extracellular compartments, as well as active transport and flow[13]. During treatment, the increase in necrosis, loss of cell membrane integrity, decrease in tumour cellularity, and increase in extracellular spaces determine the increase in water diffusion and, consequently, the increase in ADC values[14]. However, it should be mentioned that a transient decrease in ADC may occur during the first 36–48 h after starting therapy with vascular targeting agents, and the rationale may be the activation of a local immune response, as demonstrated in animal models[15]. Since DWI/ADC provides *in vivo* structural information of tissue composition at any time, and tissue composition influences the treatment response, several authors have investigated the role of this MRI technique in predicting or assessing very early therapy response in patients with CRLMs[16-21]. Most of them are concordant that pre-treatment lower ADC is associated with a better response in CRLMs patients, while a higher ADC is associated with a poorer response[16-18,20]. In particular, Cui *et al*[17] evaluated 11 patients with CRLMs and found that the pre-chemotherapy mean ADC values was significantly lower in responding lesions than those in non-responding lesions ($0.948 \pm 0.147 \times 10^{-3}$ mm^2/s *vs* $1.185 \pm 0.275 \times 10^{-3}$ mm^2/s; $P = 0.003$). Furthermore, Koh *et al*[16] analysed 20 patients with 40 CRLMs and observed that high pre-treatment ADC was predictive of poor response to oxaliplatin- and 5-fluorouracil-base chemotherapy (non-responders: 1.55×10^{-3} mm^2/s; responders: 1.36×10^{-3} mm^2/s; $P < 0.001$). These results were confirmed by Tam *et al*[18] and Fouladi *et al*[20]. The former conducted a study on a larger population composed of 102 patients with CRLMs treated with chemotherapy alone or associated with surgery/radiofrequency ablation (non-responders: 1.40×10^{-3} mm^2/s; responders: 1.16×10^{-3} mm^2/s; $P = 0.024$)[18]. The latter tested the usefulness of baseline 3D ADC to identify the potential responding CRLMs (non-responders: $1332.3 \pm 384.6 \times 10^{-6}$ mm^2/s; responders: $1150.2 \pm 272.9 \times 10^{-6}$ mm^2/s; $P = 0.04$)[20]. Recently, Uutela *et al*[22] investigated the correlation between ADC values at baseline and the RECIST response in a prospective study conducted in 52 patients with CRLM. ADC values below the median of 1.20×10^{-3} mm^2/s at baseline were associated with partial response according to the RECIST criteria 8–12 wk after starting therapy[22].

The biological rationale of these results can be postulated as follows: A higher ADC is observed in necrotic tissues, whereas a lower ADC is observed in viable areas. Necrosis before therapy may indicate a more aggressive phenotype and compromise the delivery of chemotherapeutic drugs; therefore, necrotic areas are usually poorly perfused and tumour cells are exposed to a more hypoxic and acidic environment. These factors reduce the effectiveness of the therapy[23]. However, it should be highlighted that coagulative necrosis does not increase the ADC, which could explain non-responding lesions with lower ADC[16]. In contrast, viable areas are usually well-perfused, facilitating the delivery and retention of anticancer agents.

Currently, there is no consensus regarding the optimal cutoff point ADC value for predicting response to treatment. The most important factors that influence the identification of a generally accepted ADC threshold are several, such as different scanners, methods of acquisition, sequence parameters, and choice of b values. The b-value is a factor that reflects the strength and timing of the gradients used to generate DWI images: The higher the b-value, the stronger the diffusion effect. Koh *et al*[16] identified a mean pre-treatment ADC value of 1.69×10^{-3} mm^2/s for CRLMs that did not respond to chemotherapy with a sensitivity of 60% and a specificity of 100%, whereas Fouladi *et al*[20] proposed the baseline 3D-ADC value as the optimal cut-off point of 1.006×10^{-3} mm^2/s with a sensitivity of 77.4% and a specificity of 91.3%. In this setting, Drewes *et al*[11] conducted a meta-analysis and identified a practical ADC threshold value of 1.2×10^{-3} mm^2/s, below which nearly all responders are situated and no simultaneous overlap with non-responders exists.

Although, according to the aforementioned results, ADC could appear to be a promising predictive biomarker, some studies contradict these previous results[19,21]. Matsushima *et al*[19] did not find a significant difference in ADC values between responders and non-responders to CRLMs treated with bevacizumab. Boraschi *et al*[21] correlated pre-chemotherapy ADC values of 58 CRLMs with histological tumour regression grade (TRG). TRG is a histological descriptive system aimed at grading fibrotic transformation induced in tumours by neoadjuvant therapy. In detail, TRG 1 is represented by fibrosis with no evidence of residual tumour (*i.e.* complete regression), TRG 2 is represented by fibrosis with single cells or rare groups of residual tumour cells, TRG 3 is represented by fibrosis and residual tumour with a dominance of fibrosis, TRG 4 is represented by fibrosis and residual tumour with a dominance of tumour, and TRG 5 is represented by extensive tumour without evidence of regression[24,25]. A non-linear distribution was observed between pre-ADC values and TRG; lower pre-ADC values correlated with TRG 2-3, but an overlap was observed between TRG 1 (complete response) and TRG 4-5 (no response). The heterogeneous structure of liver metastases in terms of cellularity, necrosis, and/or calcification may explain these results.

Finally, the potential role of ADC in the early prediction of therapy response in CRLMs was also evaluated. Cui *et al*[17] observed an increase in ADCs on day 3 or 7 after initiating chemotherapy in responders, suggesting a very early change in tissue composition from a more cellular pre-treatment phenotype to a less cellular or necrotic posttreatment phenotype. Knowledge of therapy effectiveness as soon as possible allows clinicians to prevent overtreatment of non-responder patients, thus avoiding adverse effects.

Intravoxel incoherent motion and diffusion kurtosis imaging

The ADC value is calculated by a mono-exponential relationship between the DWI signal and b-value. Hence, ADC is influenced by tumour heterogeneity and the Gaussian movement of water molecules. The heterogeneity of tumour tissues affects the non-Gaussian diffusion behaviour of water molecules; therefore, new non-mono-exponential diffusion models, such as intravoxel incoherent motion (IVIM) and diffusion kurtosis imaging (DKI), have been proposed to better characterise neoplastic tissues. IVIM assesses both diffusion and microcapillary perfusion changes in tissues by analysing the signal decay curve obtained from multiple b values and provides both diffusion-related parameters, such as the true diffusion coefficient (D) and ADC, and perfusion-related parameters, such as the pseudodiffusion coefficient (D*) and perfusion fraction (f)[26]. DKI estimates and quantifies the skewed distribution of water diffusion based on a probability distribution function[27]. In addition to the diffusion coefficient, DKI extracts the kurtosis value (K) that results from the probability of the diffusion displacement distribution, which is a dimensionless metric. These advanced MRI diffusion techniques have been investigated for predicting the treatment response in patients with CRLM[26,28,29]. Zhang *et al*[29] conducted a prospective study of 40 patients with CRLMs to evaluate the performance of DWI, IVIM, and DKI in predicting therapy response. Their results confirmed the promising role of ADC and suggested the potential role of IVIM and DKI. At baseline, lower ADCs and D on the IVIM parameter map, mean diffusion values, and higher K values on the DKI parameter map correlated with a better response (P = 0.001, < 0.001, = 0.003, = 0.002, respectively), with areas under the curve (AUCs) of 0.845, 0.832, 0.819, and 0.787, respectively. ADC reached the highest AUC (0.845) with a sensitivity of 73.3%, specificity of 84.0%, and cut-off value of 1.107×10^{-3} mm^2/s. In the literature, D is reported to positively correlate with the degree of tumour necrosis as well as ADC; hence, lower D is expression of poor presence of necrosis and better response to chemotherapy[30]. The combination of the aforementioned parameters by logistic regression yielded an AUC of 0.867[29]. Furthermore, Zhou *et al*[28] found that K values were higher in patients with non-responding CRLMs (responders 0.77 ± 0.15 *vs* non-responders 0.90 ± 0.15; P = 0.015), as expression of more complex microstructure, composed of micro-necroses, fibroses, and cystic changes. Finally, Kim *et al*[26] observed a significant change in diffusion parameters of IVIM, such as ADC and D, after the first cycle of therapy in responder patients, whereas perfusion-related IVIM parameters did not change significantly in both groups, suggesting that diffusion-related IVIM parameters are more useful than perfusion-related parameters in differentiating early responders from non-responders, avoiding overtreatment of patients who may not benefit from chemotherapy.

PA BASED ON SPECTROSCOPY

MR spectroscopy (MRS) is an advanced imaging technique that allows for the non-invasive measurement of the levels of some molecules *in vivo*, using the magnetic properties of certain atomic nuclei, such as protons (^{1}H), phosphorus (^{31}P), and carbon-13 (^{13}C)[31]. Therefore, MRS can provide information on tumour pathophysiology and metabolism, potentially influencing treatment planning[32]. Currently, very few studies have investigated the role of MRS in the assessment and prediction of treatment response in patients with CRLMs with poor and discordant results[22,31,33]. In ^{31}P MRS, an increased ratio of phosphomonoesters and nucleoside triphosphate is associated with tumour progression, while it decreases with tumour regression, even in the absence of changes in standard imaging[31]. These results may encourage the use of MRS in monitoring treatment response. Similarly, Kamm *et al*[33] observed a correlation between the maximum levels of 5-FU catabolites on ^{19}F-MRS and the response to treatment in patients with larger CRLMs, suggesting a potential role of MRS in the prediction of therapy response. In contrast, Uutela *et al*[22] did not find a significant association between baseline levels of free choline on ^{1}H-MRS and treatment response according to the RECIST criteria. Therefore, the role of this technique in patients with CRLMs remains to be investigated. Currently, MRS is not yet applied in clinical settings because of technical issues such as the relatively long scan times needed for a good signal-to-noise ratio, as well as the need for additional hardware and expertise in spectral interpretation.

PA BASED ON CONTRAST-ENHANCED CT OR MRI

Neoangiogenesis is induced by the upregulation of vascular growth factors and is required for tumour growth. This leads to the development of a new, altered, and immature microcirculatory network inside

the tumour lesions. The irregular vascular pattern promotes the coexistence of areas of low vascular density and areas of high angiogenic activity; consequently, regions of high cell density and necrotic, haemorrhagic, and myxoid changes are observed. The use of contrast medium and the acquisition of CT or MRI images before and after its intravenous injection allows the assessment of the vascularity of biological tissues *in vivo*, hence the tumours' neoangiogenesis. Tissue contrast enhancement can be evaluated using two different CT or MRI imaging modalities. One is dynamic and is based on repeated high-frequency image acquisition, which allows the assessment of changes in density on CT or signal intensity on MRI over time. The other is based on image acquisition at a fixed time point to obtain at least two or three phases (arterial, portal, and delayed). A broad spectrum of quantitative parameters can be extracted using dynamic acquisition images, which reflect tumour vessel features (perfusion, permeability, and density), extracellular-extravascular space composition, and plasma volume. A summary of the main quantitative parameters used in the assessment of treatment response in patients with CRLM is presented in Table 1. The development of targeting agents with angiogenesis-inhibiting effects, such as bevacizumab, has encouraged studies to examine the correlation between angiogenesis and quantitative imaging parameters. Currently, several potential predictive imaging biomarkers have been identified in different types of cancers, such as renal cell carcinoma, hepatocellular carcinoma, hypopharyngeal carcinoma, and colorectal cancer[10,34-36].

Contrast-enhanced MRI

Few studies have been published regarding the predictive role of MRI quantitative perfusion parameters in patients with CRLMs[37-41]. In particular, Coenegracht *et al*[37] observed in 10 patients with CRLMs a significant difference of K^{ep} values between responders and non-responders (0.09852 *vs* 0.07829; $P < 0.001$); O'Connor *et al*[41] also noticed a high ratio of enhancing tumour voxels to overall tumour voxels in patients with better tumour response. The pathophysiological basis of these results should be as follows: Higher baseline K^{ep} values indicate higher exchange of contrast medium between the blood and the extracellular extravascular space; similarly, a higher exchange of chemotherapy may occur. For this reason and for the presence of an oxygen-rich environment, highly perfused CRLMs at baseline are more likely to respond well to treatment. Furthermore, the role of MRI quantitative perfusion parameters in the prediction of treatment response in patients with CRLMs after the first cycle of a chemotherapy regimen containing bevacizumab has also been investigated. Hirashima *et al*[38] observed a correlation between a higher response and the decrease in K^{trans} ratio (ΔK^{trans}) and K^{ep} ratio (ΔK^{ep}), calculated at baseline and after the first cycle ($P < 0.0001$). De Bruyne *et al*[40] found a correlation between worse response and an increase of at least 40% in K^{trans} after the first cycle of treatment. These results suggest a potential role for quantitative dynamic contrast-enhanced MRI (DCE-MRI) parameters in the early prediction of therapy response and in the assessment of drug resistance[38,40]. On the other hand, Kim *et al*[39] observed discordant results; no significant change in perfusion parameters, such as K^{trans}, K^{ep} and V_e, was found after the first cycle of chemotherapy between responders and non-responders, questioning their role in predicting early therapy response in CRLMs patients.

In clinical practice, gadoxetic acid, a hepatobiliary contrast agent incorporated into hepatocytes by the transporter OATP1B3, is used to better assess CRLMs because of the excellent lesion-to-liver contrast of the hepatobiliary phase (HBP). Murata *et al*[42] investigated the role of gadoxetic acid-enhanced MRI in predicting treatment response in patients with CRLMs. The authors calculated the pre-treatment relative tumour enhancement of the HBP (RTE_{HBP}) in 26 patients with CRLMs using the following formula: RTE values (%) = $[(SI_H - SI_P)/SI_P] \times 100$, where SI_H and SI_P are the signal intensities in the hepatobiliary and pre-contrast phases, respectively. The mean pre-treatment RTE_{HBP} values were significantly higher in responders than in non-responders (37.2% ± 10.9% *vs* 17.9% ± 10.5%; $P = 0.0006$), suggesting a potential association between chemotherapeutic response and OATP1B3 expression. OATP1B3 is an organic anion transporter that is incorporated into hepatocytes, not only in gadoxetic acid, but also in endogenous and exogenous molecules, such as bile acids and chemotherapeutic agents.

Contrast-enhanced CT

CRLMs are generally hypovascular lesions in the portal phase that obtain their blood supply primarily from the hepatic artery; hence, they are arterialised tumours with increased blood flow (BF) and vascular permeability[43]. Based on this assumption, Joo *et al*[44] investigated the haemodynamic features of liver metastases using quantitative colour mapping of the arterial enhancement fraction (AEF) to explore its potential role in the prediction of therapeutic response in patients with CRLMs. The Authors observed a higher mean AEF value of metastatic tumour (58.9 ± 18.8) than that of tumour-adjacent parenchyma (35.5 ± 15.4) and tumour-free parenchyma (26.4 ± 7.5) (all $P < 0.0001$), confirming the arterial vascularisation of liver metastases. Similarly, Kim *et al*[45] extracted some perfusion parameters from perfusion CT of 17 patients with CRLMs and noticed that BF, K^{trans}, and portal liver perfusion were significantly lower in metastatic lesions than in background normal liver parenchyma (41.2 *vs* 50.8, 25.9 *vs* 41.2, 19.3 *vs* 40.9 mL/100 mL/min, respectively), while arterial CRLM perfusion indices were significantly higher than those of hepatic perfusions (28.0 *vs* 22.9 mL/100 mL/min and 57.1% *vs* 26.6%, respectively) ($P < 0.05$). The metastatic blood supply from the hepatic artery and their increased arterial perfusion may be due to the development of a microcirculatory network caused by the neoangiogenesis process. As a consequence, responding lesions of CRLMs patients showed significantly

Table 1 Main quantitative parameters extracted from perfusion computed tomography and magnetic resonance imaging imaging techniques to predict treatment response in patients with colorectal liver metastasis		
Parameter name	Parameter definition	Parameter significance
Transfer constant (K^{trans})	Rate of contrast extraction from the blood to the interstitium	It reflects the balance between capillary permeability and BF in a tissue
Tissue interstitial volume (V^e)	Volume of extravascular and extracellular contrast agent in a certain tissue, expressed as a percentage	It is a measure of cell density
Rate contrast (K^{ep})	Rate at which the contrast agent returns from the extravascular-extracellular space to the vascular compartment ($K^{ep} = K^{trans}/V^e$)	It reflects the tissue microcirculation and contrast agent permeability
Regional BF	BF *per* unit volume or mass of tissue (mL of blood/min/100 mL of tissue)	It expresses the rate of the delivery of nutrients and oxygen to a certain tissue

BF: Blood flow.

higher AEF values than that non-responding (65.5 ± 9.6 *vs* 51.3 ± 13.2; *P* = 0.005)[44]. These results are concordant with those of Osawa *et al*[46], who investigated the predictive role of contrast-enhanced CT in patients with CRLM treated with chemotherapy with or without bevacizumab. The authors found a significant correlation between a higher composite endpoint (CE) ratio (ratio of CT value during the arterial phase to unenhanced CT value) at baseline and higher tumour shrinkage after four cycles of chemotherapy associated with bevacizumab (R^2 = 0.24, *P* = 0.03), unlike in patients not treated with bevacizumab. Furthermore, among CRLM patients with a high CE ratio at baseline, an increase of 29.6% in the tumour shrinkage rate was observed in those treated with bevacizumab compared with a decrease of 1.46% in those not treated with bevacizumab (*P* = 0.03). Among the CRLMs patients with a low CE ratio at baseline, no significant tumour shrinkage was noted. The rationale for these results is unclear, but we can hypothesise that the presence of higher microvessel density at baseline, evaluated on CT as higher AEF values or higher CE ratios, promotes greater delivery of chemotherapeutic agents. Hence, the assessment of these parameters at baseline could be useful in the prediction of treatment response and drug resistance in patients with CRLMs.

Finally, although Kim *et al*[45] did not find any significant difference in perfusion parameters at baseline between responder and non-responder patients with CRLMs, they observed a significant decrease in BF and K^{trans} after the first cycle of chemotherapy (BF: 28.3% *vs* 5.2%, *P* = 0.036, AUC: 0.806; K^{trans}: 18.7% *vs* 13.0%, *P* = 0.027, AUC: 0.819). The early reduction in perfusion parameters may reflect the inhibiting effect of neo-angiogenesis by anticancer drugs and should encourage clinicians to continue the chosen chemotherapy regimen. Furthermore, the Authors identified a cut-off value for the reduction rate of K^{trans} of 15.0% after the first cycle of chemotherapy, with a sensitivity of 66.7% and specificity of 87.5%[45].

PA BASED ON HYBRID IMAGING

The 2-[^{18}F]FDG-PET/CT and 2-[^{18}F]FDG-PET/MRI are molecular and morphological imaging techniques associated with metabolic and anatomical evaluation of tumour lesions[47,48]. The tracer 2-[^{18}F]FDG, an analogue of glucose, is injected intravenously, transported into cells through membrane glucose transporter proteins, and tends to accumulate in malignant cells because of increased glucose consumption[49]. The uptake of 2-[^{18}F]FDG detected by PET can be quantitatively assessed using different parameters; the main parameters used in the prediction of therapy response in CRLMs patients are shown in Table 2[45,48].

Currently, the quantitative evaluation of tumour metabolism using 2-[^{18}F]FDG-PET integrated with CT or MRI plays a crucial role in the routine management of oncological patients. In patients with colorectal cancer, hybrid imaging aids in the detection of extrahepatic distant metastasis in the evaluation of therapy response, as well as in the follow-up of treated patients with rising serum carcinoembryonic antigen (CEA) levels and no detectable disease on morphological imaging[48]. To date, the role of this hybrid technique in the prediction of treatment response in CRLMs patients remains under investigation. Several studies have shown that standardised maximum uptake value (SUV_{max}) is significantly lower in responders than in non-responders before chemotherapy with or without bevacizumab[10,40,45,50-52]. In detail, Byström *et al*[50] found a mean baseline SUV_{max} of 5.6 in responders and 7.4 in non-responders treated with irinotecan-based chemotherapy (*P* = 0.02). Similarly, De Bruyne *et al*[40] observed a mean baseline SUV_{max} of 3.77 in responders and 7.20 in non-responders treated with FOLFOX/FOLFIRI and bevacizumab followed by surgery (*P* = 0.012). In addition, De Bruyne *et al*[40] did not find any correlation between DCE-MRI parameters, SUV_{max} and anatomical tumour response, suggesting that tumour BF, glucose metabolism, and shrinkage are potentially

Table 2 Main quantitative parameters extracted from the 18-fluorodexoyglucose positron emission tomography used in the prediction of treatment response in patients with colorectal liver metastasis

Parameter name	Parameter definition
SUV_{max}	Uptake value of the pixel with the highest activity inside an ROI divided by the injected dose, which must be corrected for decay and normalised to the patient's weight or body surface
SUV_{mean}	Average of all the uptake values of the pixels within an ROI
MTV	Volume of tumour tissues included in a tridimensional ROI with pathological FDG uptake *via* threshold represented by a settled absolute value or percentage of the SUV_{max} or SUV_{mean}
	It includes both volumetric data and metabolic activity of the tumour
TLG	The product of multiplying SUV_{mean} by MTV
SAM	A marker of total lesion glycolysis, calculated by drawing a volume of interest [VOI(1)] around the tumour and a larger VOI [VOI(2)] around VOI(1)
	SAM = Total SUV VOI1 − (mean BG × volume VOI1)
	Mean BG (background activity) = (total SUV VOI2 − total SUV VOI1)/(volume VOI2 − volume VOI1)

SUV_{max}: Standardised maximum uptake value; SUV_{mean}: Standardised mean uptake value; MTV: Metabolic tumour volume; TLG: Total lesion glycolysis; SAM: Standardised added metabolic activity; FDG: Fluorodexoyglucose; PET: Positron emission tomography; ROI: Region of interest; VOI: Volume of interest.

independent predictors[40]. Mertens *et al*[53] introduced a new metabolic parameter, the standardised added metabolic activity (SAM), which is a marker of total lesion glycolysis that measures the total excess tumoural SUV above the tumour background (Table 2). The authors found a significant difference in both SAM and SUV_{max} at baseline between responders and non-responders (34 *vs* 211, P = 0.002; 3.8 *vs* 7.2, P = 0.021, respectively)[52].

In addition to SUV_{max}, other metabolic parameters have been proposed as predictors of therapy response in patients with CRLMs, such as standardised mean uptake value (SUV_{mean30}), metabolic tumour volume (MTV_{30}) and 30% lesion glycolysis (LG_{30}). SUV_{mean30} was defined as the average value of the SUV of the voxels that showed $SUV_{max} \geq 30\%$. MTV_{30} was defined as the tumour volume segmented *via* the threshold SUV_{mean30} of the lesion. Finally, LG_{30} was obtained by multiplying MTV_{30} by SUV_{mean30}. Kim *et al*[45] observed a higher mean SUV_{mean30} in responder than in non-responder patients with CRLMs on prechemotherapy 2-[18F]FDG-PET/CT (5.2 ± 2.3 *vs* 3.5 ± 1.0, P = 0.046; AUC: 0.792) and a significant difference in the reduction rate of MTV_{30} and LG_{30} between responders and non-responders (18.1% *vs* -5.5%, P = 0.015, AUC: 0.847; 37.9% *vs* 10.7%, P = 0.008, AUC: 0.868, respectively) on 2-[18F]FDG-PET/CT performed 2 or 3 wk after the first cycle of chemotherapy. These results suggest the role of these other 2-[18F]FDG-PET/CT quantitative parameters in the prediction of treatment response in patients with CRLMs. In the same population, Kim *et al*[45] did not observe a significant reduction in the SUV_{max} after the first cycle of therapy between responders and non-responders. A possible explanation is that SUV_{max} is based only on a single pixel and does not consider the entire heterogeneous tumour volume, whereas MTV and LG are volume-based parameters and could be more accurate in the early prediction of treatment response. Similarly, Hendlisz *et al*[51] investigated the potential role of 2-[18F]FDG-PET/CT in the prediction of early response after the first cycle of chemotherapy in patients with CRLMs. To avoid metabolic imaging-based rejection of potentially beneficial therapy, the lowest possible reliable response threshold for FDG uptake changes, the $\Delta SUV_{max} < 15\%$, was applied. Using this threshold, the predictive performance of the metabolic assessment for RECIST response showed a sensitivity of 100%, specificity of 57%, positive predictive value of 43%, and negative predictive value of 100%.

Finally, in the assessment of early response to chemotherapy with 2-[18F]FDG-PET, the flare phenomenon should be considered because it might interfere with the measurement of quantitative parameters. It occurs–1–2 wk after the initiation of chemotherapy and consists of a marked increase in 2-[18F]FDG metabolism in lesions that respond later. Hence, it is recommended to avoid the first two weeks after chemotherapy when performing 2-[18F]FDG-PET/CT evaluation[54].

PA BASED ON RADIOMICS

Radiomics represents a multi-step post-processing technique that can be applied to any medical image to convert it into mineable high-dimensional data (radiomics features). The assumption is that biomedical images contain information that reflects tissue heterogeneity and pathophysiology[8]. Radiomics data can be used alone or with other clinical data to build predictive models and decision-

support tools to aid physicians in clinical practice, potentially improving diagnostic, prognostic, and predictive accuracy. Radiomics analyses represent the pursuit of precision medicine to choose the right treatment for the right patient at the right time. To extract the radiomics features, the first step is image acquisition; the second step is image segmentation, which consists of the 2D or 3D delineation of the ROI, represented by the largest cross-section of the tumour, the whole tumour, or tumour sub-regions; and the third step is the radiomics data extraction (Figure 2). Radiomics features are obtained from the drawn ROI using specifically designed formulae conveying different quantitative parameters, such as first-order (based on histogram analysis of the distribution of individual voxel values without concern for spatial distribution) and second- and higher-order statistical descriptors (accounting for pixel intensity spatial distribution)[55]. Second-order statistical descriptors are generally defined as "texture" features, which describe the statistical interrelationship between voxels with similar or dissimilar contrast values, providing a measure of heterogeneity.

The huge amount of radiomics data extracted from medical images can be more easily handled by artificial intelligence (AI) than traditional statistical methods, and machine learning (ML) is a branch of AI focused on algorithms that can be trained for a task they were not specifically programmed to perform[56]. The algorithms are decision support tools and are mainly used for classification problems. In the oncological field, they are applied to detect and characterise tumour lesions as well as to predict and monitor therapy response. A family of ML algorithms of particular interest is represented by neural networks (NN), a complex model composed of nodes (called neurones) that contribute to the creation of deep, multi-layered networks. The use of NNs with such architectures is commonly referred to as deep learning (DL), which autonomously learns the best features for performing data classification[56]. The texture features utilised were a grey-level co-occurrence matrix (GLCM) and grey-level run length (GLRL). Some features were extracted after pre-processing with a wavelet transform. Supervised classification was achieved using ML approaches: Support vector machine (SVM), k-nearest neighbours, and Random Forest. Texture analysis (TA) is a technique that enables the quantification of variations in pixel intensity, including those imperceptible to the human visual system. TA includes the quantification of grey-level patterns, pixel interrelationships, and the spectral properties of an image[57,58].

Few studies have been published on the role of radiomics applied to CT and MRI images to predict therapy response in patients with CRLMs[59-64].

MRI

Zhang *et al*[63] conducted an analysis of T2-weighted images of liver MRI in 26 patients with CRLMs (a total of 193 liver metastases) and extracted five histogram features (mean, variance, skewness, kurtosis, and entropy) and five GLCMs, including angular second moment (ASM), entropy, contrast, correlation, and inverse difference moment. Among the former parameters, only variance was significantly different between CRLMs responders and non-responders ($P < 0.001$), whereas among the latter, all parameters were significantly different ($P \leq 0.001$). Furthermore, when tested using multivariable logistic regression analysis, the association of variance and ASM showed the most potential predictive value for discriminating responders from non-responders with an AUC of 0.814, a sensitivity of 71%, and a specificity of 84.9. These parameters correlate with the complexity and non-uniformity of the image texture, and hence with tumour heterogeneity. According to Zhang *et al*[63], heterogeneous tumours seem to have a more favourable response to therapy. This observation may be related to irregular angiogenesis, greater distribution of tumour blood vessels, and extracellular vascular permeability. Since the effect of drugs relies on their delivery to the tumour site, tumours with greater heterogeneity should theoretically have a better response.

Furthermore, Liang *et al*[62] performed a histogram analysis using ADC maps of 53 patients with CRLMs before starting chemotherapy and observed that the mean, 1st, 10th, 50th, 90th, and 99th percentile values of the ADC maps were significantly lower in responders than in non-responders ($P = 0.000-0.002$) with AUCs of 0.79, 0.76, 0.76, 0.79, 0.80, and 0.82, respectively. The 99th percentile of ADC showed the highest diagnostic performance for predicting response to chemotherapy, with an AUC of 0.82. These results are concordant with those mentioned above: ADC values included in the 99th percentile are predictive of a good response to chemotherapy, suggesting their association with viable neoplastic tissues, whereas the remaining 1% of ADC values are predictive of insensitivity to chemotherapy, suggesting their association with areas of fluid resulting from necrotic tissues. The authors also investigated histogram-derived CE-MRI parameters extracted from arterial and portal venous phases, such as mean, variance, skewness, kurtosis, and 1st, 10th, 50th, 90th, and 99th percentiles; however, they did not find any significant difference between responders and non-responders in patients with CRLMs. These results may reflect the fact that tumour enhancement is non-specific and influenced by several factors, including BF, capillary permeability, blood volume, and extravascular leakage space[62].

CT

Ahn *et al*[59] conducted a study of 235 patients (145 in the training cohort and 90 in the validation cohort) with CRLMs treated with FOLFOX and FOLFIRI to evaluate several parameters on contrast-enhanced CT, including histogram, volumetric, and morphological features. In multivariate analysis, lower skewness [odds ratio (OR): 6.739, $P = 0.003$] in 2D analysis, higher mean attenuation (OR: 2.587, $P = 0.017$), and narrower standard deviation (SD) (OR: 3.163, $P = 0.002$) in 3D analysis attained statistical

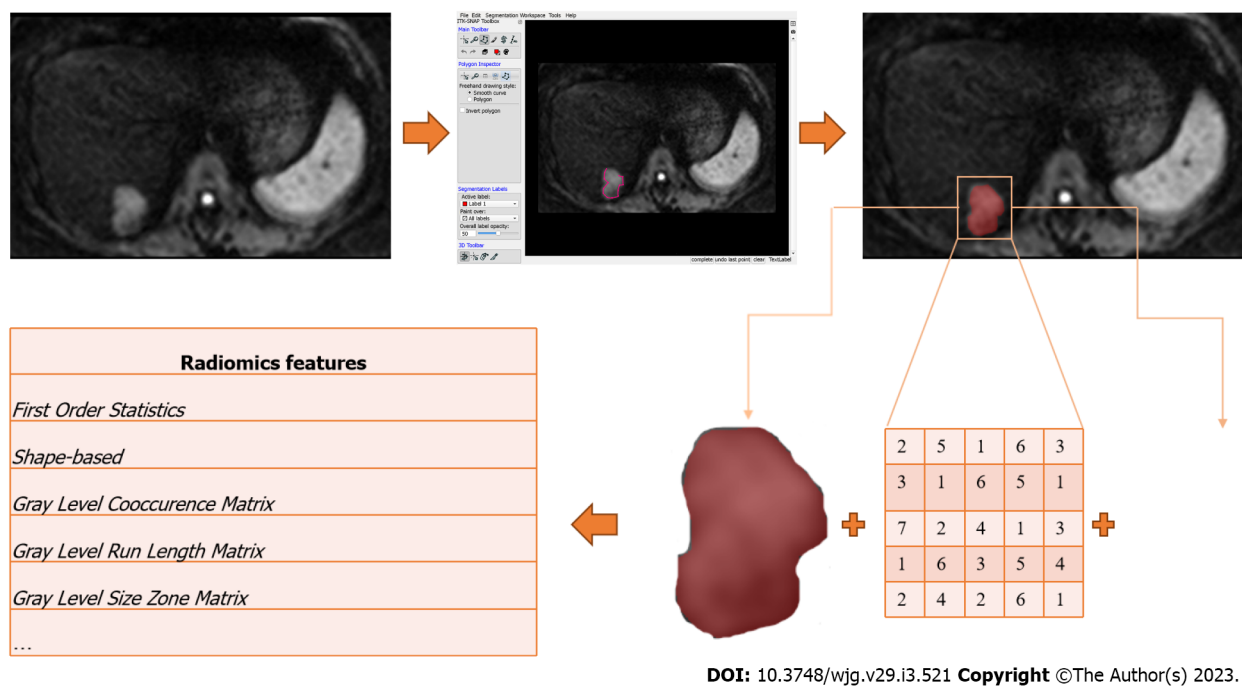**DOI:** 10.3748/wjg.v29.i3.521 **Copyright** ©The Author(s) 2023.

Figure 2 Schematic diagram showing how radiomics features can be extracted from medical images using a diffusion-weighted imaging image from an magnetic resonance imaging scan of a patient with colorectal liver metastasis as an example. The process begins on the left upper corner with image acquisition, followed by lesion segmentation on a dedicated software leading to a region of interest. The shape of the region of interest as well as the distribution and spatial relation of intensity values of each pixel are computationally analysed to extract radiomics features of different order.

significance for predicting the response of CRLMs to chemotherapy in the training cohort. The lower skewness on 2D images and the narrower SD on 3D images showed good performance in the validation cohorts (AUC: 0.797 and 0.785, respectively). In contrast, Rabe *et al*[64] conducted a CT TA on 29 patients with non-necrotic CRLMs and did not observe a significant correlation between SD and the prediction of response. A possible explanation for these contradicting results could be the exclusion of necrotic lesions in the analysis conducted by Rabe *et al*[64]; indeed, necrosis increases SD. Furthermore, among the several first- and second-order radiomics features extracted by Rabe *et al*[64], eight, such as minimum histogram gradient intensity, skewness, discretised skewness, volume at intensity fraction 10, three GLRL indicators (long run low grey level emphasis, low grey level run emphasis, short run low grey level emphasis), and low grey level count emphasis, were significantly associated with treatment response in univariate analysis. Due to strong correlations within these radiomics features, only two, minimum histogram gradient intensity and long-run grey level emphasis, were included in the multivariate analysis. The AUC of the multivariate model using minimum histogram gradient intensity and long-run grey level emphasis was 0.80, with a sensitivity of 0.73 and a specificity of 0.79 reached with the best threshold of the linear predictor of 0.42. In addition, Ravanelli *et al*[60] investigated the role of contrast-enhanced CT TA in predicting treatment responses to chemotherapy ± bevacizumab in 43 patients with CRLMs. Uniformity was lower in responders than in non-responders ($P < 0.001$) in the bevacizumab-containing chemotherapy group, and in the multivariate analysis, this parameter was independently correlated with radiological CT response at three months (OR: 20, $P = 0.01$). The CT texture parameters were not significantly different between responders and non-responders in the group of patients treated with chemotherapy alone. The correlation between lower uniformity and responders to chemotherapy regimens containing bevacizumab seems to contradict the concept that higher heterogeneity reflects greater aggressiveness. However, it should be highlighted that lesion uniformity is mainly influenced by the presence of angiogenesis, which is triggered and promoted by the upregulation of VEGF, the molecular target of bevacizumab; indeed, the leakage of contrast medium from newly formed and highly permeable tumour microvessels into the extracellular space could account for the small areas of hyper-enhancement that are quantified by the variable uniformity. Hence, the assessment of uniformity should be useful in clinical practice for identifying patients who may benefit from bevacizumab. Low contrast-enhanced CT lesion density was significantly associated with no response in patients with CRLMs treated with chemotherapy with or without bevacizumab ($P = 0.03$ and 0.02, respectively), reflecting poor vascularisation, and thus poor local bioavailability of chemotherapy. Creasy *et al*[61] evaluated, for the first time, the prediction of volumetric response to systemic chemotherapy alone or in association with hepatic artery infusion (HAI), extracting 272 radiomics features from the largest hepatic metastases of 157 colorectal cancer patients. Thirty of the 271 analysed CT radiomics features were selected based on the univariate analysis and used as inputs for

the multivariate regression model. This model was constructed to calculate the percentage of tumour responses. The mean absolute prediction error (MAPE), which represents the mean difference between the predicted response from the model and actual radiographic response, was calculated. MAPE was 16.5% for the training set and 21.5% for the validation set. Furthermore, they conducted a secondary analysis in the validation set stratified by HAI utilisation, demonstrating a MAPE of 19.5% for patients with CRLM treated with HAI and 25.1% for those treated with chemotherapy alone. Since HAI chemotherapy is an expensive treatment with potential complications, predicting the response before starting therapy is very useful for clinicians to choose the most appropriate treatment strategy for each patient.

In the era of personalised medicine, Giannini *et al*[65] developed and validated an ML algorithm to predict the response of individual liver metastases in 24 colorectal cancer patients with a total of 123 lesions, extracting 22 radiomics features on pre-treatment portal CT scans and using an SVM classifier. Their ML algorithm achieved accuracies of 80.9% and 61.5% with sensitivities of 85.7% and 72.7%, and specificities of 66.7% and 47.1%, in the training and test sets, respectively. The prediction of response for each metastasis is crucial in treatment planning because the detection of one or more metastases that will respond differently than others can suggest clinicians to treat them differently[65]. The same group of researchers developed another ML algorithm to predict response in a subgroup of patients with CRLMs and who express HER2 amplification and undergo HER2-targeted therapy[66]. These patients may exhibit a heterogeneous response because some metastases shrink, while others progress[67]. Giannini *et al*[66] extracted 24 radiomics features from a 3D-ROI drawn on baseline portal phase CT and used a Gaussian naïve Bayesian classifier. The radiomics score of individual metastases reached a per-lesion sensitivity of 90% and specificity of 42% in the validation set; thus, the ML algorithm was more accurate in predicting responders than non-responders.

Wei *et al*[68] developed and validated a DL-based radiomics model based on contrast-enhanced CT to predict the response to chemotherapy in patients with CRLMs. The authors compared the diagnostic accuracy of four predictive models based on clinical data and contrast-enhanced CT qualitative features, such as tumour margin, enhanced rim, and target lesion size, DL-based radiomics model, and a combined model. The model that reached the highest AUC was constructed using a combination of CEA level and DL-based fusion radiomics signature (AUC of 0.935 in the training cohort and 0.830 in the validation cohort). Considering that the scanning CT parameters may influence the grey level values and, consequently, the radiomics features, Ahn *et al*[59] compared data acquired with four different CT scanners and did not find any significant differences.

SYNTHESIS OF CURRENT KNOWLEDGE, LIMITS AND FUTURE PERSPECTIVES

The accurate prediction of therapy response in patients with CRLMs is a clinical requirement. In this setting, different imaging techniques such as MRI, CT, and 2-[18F]FDG-PET/CT have been investigated.

PA imaging plays a crucial and promising role. However, evidence is limited, and reproducibility is a major concern. First, most of the studies were retrospective, monocentric, and conducted on small samples, and their results were not validated in the external population. Therefore, prospective, multicentre studies with a larger patient population should be conducted. On the other hand, the identification of a universally accepted cut-off value for each imaging quantitative parameter would be desirable, but it represents a great and ambitious challenge. Indeed, scanners and protocols may influence the value of some quantitative parameters such as ADC and radiomics features.

Regarding contrast-enhanced MRI and CT, perfusion parameters showed the most promising results for predicting therapy response in patients with CRLM. Unfortunately, perfusion techniques have not yet been introduced in routine clinical practice, possibly because of the complexity of the parameter measurements and acquisition protocols. In addition, the quantification of contrast agent concentration is difficult because of the complex relationship between density on CT and signal intensity on MRI and contrast medium concentration, influenced by many factors, such as contrast agent dose, injection rate, time of circulation, and scanner parameters. Finally, the current tumour ROI analysis utilises mean quantitative vascular parameters, which do not accurately reflect the spatial heterogeneity of tumour perfusion.

Regarding hybrid imaging techniques, only a few studies have been published, and they recognise a promising role of 2-[18F]FDG-PET/CT in the prediction of treatment response in patients with CRLM, although this is still under investigation. This technique is not routinely performed in clinical practice, and FDG uptake is influenced by different factors such as tumour grade and histological type.

Recently the emergency of radiomics opens new horizons about the potential role of imaging techniques in predicting tumour response in patients with CRLMs, but currently a lot of issues have to be solved. First, the biological correlation of radiomics features is unclear, and second, imaging acquisition and post-processing may influence the values of radiomics features, hence their reproducibility between different centres. Radiomics represents an ongoing topic of investigation, but its clinical effectiveness remains to be defined.

Hence, considering the great potential of PA in the prediction of therapy response in patients with CRLMs, some issues should be solved. To overcome the lack of reproducibility of quantitative imaging parameters, centre-specific solutions could be hypothesised (*i.e.* each centre could identify its own threshold using the same protocol and the same scanner every time).

Finally, considering that PA is time consuming, the real effect on patient management and outcomes must be defined accurately before introducing it in clinical practice.

CONCLUSION

In an oncological setting, PA applied to cross-sectional imaging allows the extraction of numerical data from neoplastic tissues, which are correlated with morphological, structural, functional, and metabolic features. *In vivo* evaluation of parametric imaging biomarkers can estimate the likelihood of response and drug resistance in individual patients before or immediately after starting chemotherapy and targeted agent therapy. Although the potential role of different imaging quantitative parameters in the prediction of therapy response in patients with CRLMs has been investigated, there is no consensus about which is the most promising parameter; moreover, sometimes the results are controversial. This critical point depends in part on the need for standardisation of the acquisition protocols to obtain data of good quality and reproducibility among different scanners and operators, a well-defined cut-off value, and a clear knowledge of the clinical significance of each imaging quantitative parameter. Therefore, further investigation should be conducted in this field. The identification of a shared quantitative predictive imaging parameter can be of clinical value because it avoids the risk of toxicity in patients who may not benefit from treatment as well as an economic utility to reduce unnecessary healthcare costs.

FOOTNOTES

REFERENCES

1   **Väyrynen V**, Wirta EV, Seppälä T, Sihvo E, Mecklin JP, Vasala K, Kellokumpu I. Incidence and management of patients with colorectal cancer and synchronous and metachronous colorectal metastases: a population-based study. *BJS Open* 2020; **4**: 685-692 [PMID: 32543788 DOI: 10.1002/bjs5.50299]

2   **Adam R**, Kitano Y. Multidisciplinary approach of liver metastases from colorectal cancer. *Ann Gastroenterol Surg* 2019; **3**: 50-56 [PMID: 30697610 DOI: 10.1002/ags3.12227]

3   **Lam VW**, Spiro C, Laurence JM, Johnston E, Hollands MJ, Pleass HC, Richardson AJ. A systematic review of clinical response and survival outcomes of downsizing systemic chemotherapy and rescue liver surgery in patients with initially unresectable colorectal liver metastases. *Ann Surg Oncol* 2012; **19**: 1292-1301 [PMID: 21922338 DOI: 10.1245/s10434-011-2061-0]

4   **Messersmith WA**. NCCN Guidelines Updates: Management of Metastatic Colorectal Cancer. *J Natl Compr Canc Netw* 2019; **17**: 599-601 [PMID: 31117039 DOI: 10.6004/jnccn.2019.5014]

5   **Mainenti PP**, Romano F, Pizzuti L, Segreto S, Storto G, Mannelli L, Imbriaco M, Camera L, Maurea S. Non-invasive diagnostic imaging of colorectal liver metastases. *World J Radiol* 2015; **7**: 157-169 [PMID: 26217455 DOI: 10.4329/wjr.v7.i7.157]

6   **Mainenti PP**, Mancini M, Mainolfi C, Camera L, Maurea S, Manchia A, Tanga M, Persico F, Addeo P, D'Antonio D, Speranza A, Bucci L, Persico G, Pace L, Salvatore M. Detection of colo-rectal liver metastases: prospective comparison of contrast enhanced US, multidetector CT, PET/CT, and 1.5 Tesla MR with extracellular and reticulo-endothelial cell specific contrast agents. *Abdom Imaging* 2010; **35**: 511-521 [PMID: 19562412 DOI: 10.1007/s00261-009-9555-2]

7   **Eisenhauer EA**, Therasse P, Bogaerts J, Schwartz LH, Sargent D, Ford R, Dancey J, Arbuck S, Gwyther S, Mooney M, Rubinstein L, Shankar L, Dodd L, Kaplan R, Lacombe D, Verweij J. New response evaluation criteria in solid tumours: revised RECIST guideline (version 1.1). *Eur J Cancer* 2009; **45**: 228-247 [PMID: 19097774 DOI: 10.1016/j.ejca.2008.10.026]

8   **Gillies RJ**, Kinahan PE, Hricak H. Radiomics: Images Are More than Pictures, They Are Data. *Radiology* 2016; **278**: 563-577 [PMID: 26579733 DOI: 10.1148/radiol.2015151169]

9   **van Laarhoven HW**, Klomp DW, Rijpkema M, Kamm YL, Wagener DJ, Barentsz JO, Punt CJ, Heerschap A. Prediction of chemotherapeutic response of colorectal liver metastases with dynamic gadolinium-DTPA-enhanced MRI and localized 19F MRS pharmacokinetic studies of 5-fluorouracil. *NMR Biomed* 2007; **20**: 128-140 [PMID: 17006886 DOI: 10.1002/nbm.1098]

10   **Beckers RCJ**, Lambregts DMJ, Lahaye MJ, Rao SX, Kleinen K, Grootscholten C, Beets GL, Beets-Tan RGH, Maas M. Advanced imaging to predict response to chemotherapy in colorectal liver metastases - a systematic review. *HPB (Oxford)* 2018; **20**: 120-127 [PMID: 29196021 DOI: 10.1016/j.hpb.2017.10.013]

11   **Drewes R**, Pech M, Powerski M, Omari J, Heinze C, Damm R, Wienke A, Surov A. Apparent Diffusion Coefficient Can Predict Response to Chemotherapy of Liver Metastases in Colorectal Cancer. *Acad Radiol* 2021; **28** Suppl 1: S73-S80 [PMID: 33008734 DOI: 10.1016/j.acra.2020.09.006]

12   **Patterson DM**, Padhani AR, Collins DJ. Technology insight: water diffusion MRI--a potential new biomarker of response to cancer therapy. *Nat Clin Pract Oncol* 2008; **5**: 220-233 [PMID: 18301415 DOI: 10.1038/ncponc1073]

13   **Herneth AM**, Guccione S, Bednarski M. Apparent diffusion coefficient: a quantitative parameter for in vivo tumor characterization. *Eur J Radiol* 2003; **45**: 208-213 [PMID: 12595105 DOI: 10.1016/s0720-048x(02)00310-8]

14   **Moffat BA**, Chenevert TL, Lawrence TS, Meyer CR, Johnson TD, Dong Q, Tsien C, Mukherji S, Quint DJ, Gebarski SS, Robertson PL, Junck LR, Rehemtulla A, Ross BD. Functional diffusion map: a noninvasive MRI biomarker for early stratification of clinical brain tumor response. *Proc Natl Acad Sci U S A* 2005; **102**: 5524-5529 [PMID: 15805192 DOI: 10.1073/pnas.0501532102]

15   **Thoeny HC**, De Keyzer F, Chen F, Ni Y, Landuyt W, Verbeken EK, Bosmans H, Marchal G, Hermans R. Diffusion-weighted MR imaging in monitoring the effect of a vascular targeting agent on rhabdomyosarcoma in rats. *Radiology* 2005; **234**: 756-764 [PMID: 15734932 DOI: 10.1148/radiol.2343031721]

16   **Koh DM**, Scurr E, Collins D, Kanber B, Norman A, Leach MO, Husband JE. Predicting response of colorectal hepatic metastasis: value of pretreatment apparent diffusion coefficients. *AJR Am J Roentgenol* 2007; **188**: 1001-1008 [PMID: 17377036 DOI: 10.2214/AJR.06.0601]

17   **Cui Y**, Zhang XP, Sun YS, Tang L, Shen L. Apparent diffusion coefficient: potential imaging biomarker for prediction and early detection of response to chemotherapy in hepatic metastases. *Radiology* 2008; **248**: 894-900 [PMID: 18710982 DOI: 10.1148/radiol.2483071407]

18   **Tam HH**, Collins DJ, Brown G, Chau I, Cunningham D, Leach MO, Koh DM. The role of pre-treatment diffusion-weighted MRI in predicting long-term outcome of colorectal liver metastasis. *Br J Radiol* 2013; **86**: 20130281 [PMID: 23995873 DOI: 10.1259/bjr.20130281]

19   **Matsushima S**, Sato T, Nishiofuku H, Sato Y, Murata S, Kinosada Y, Era S, Inaba Y. Equivalent cross-relaxation rate imaging and diffusion weighted imaging for early prediction of response to bevacizumab-containing treatment in colorectal liver metastases-preliminary study. *Clin Imaging* 2017; **41**: 1-6 [PMID: 27721090 DOI: 10.1016/j.clinimag.2016.08.013]

20   **Fouladi DF**, Zarghampour M, Pandey P, Pandey A, Varzaneh FN, Ghasabeh MA, Khoshpouri P, Kamel IR. Baseline 3D-ADC outperforms 2D-ADC in predicting response to treatment in patients with colorectal liver metastases. *Eur Radiol* 2020; **30**: 291-300 [PMID: 31209620 DOI: 10.1007/s00330-019-06289-3]

21   **Boraschi P**, Donati F, Cervelli R, Pacciardi F, Tarantini G, Castagna M, Urbani L, Lencioni R. Colorectal liver metastases: ADC as an imaging biomarker of tumor behavior and therapeutic response. *Eur J Radiol* 2021; **137**: 109609 [PMID: 33647779 DOI: 10.1016/j.ejrad.2021.109609]

22   **Uutela A**, Ovissi A, Hakkarainen A, Ristimäki A, Lundbom N, Kallio R, Soveri LM, Salminen T, Ålgars A, Halonen P, Ristamäki R, Nordin A, Blanco Sequeiros R, Rinta-Kiikka I, Lantto E, Virtanen J, Pääkkö E, Liukkonen E, Saunavaara J, Ryymin P, Lammentausta E, Osterlund P, Isoniemi H; RAXO Study Group. Treatment response of colorectal cancer liver metastases to neoadjuvant or conversion therapy: a prospective multicentre follow-up study using MRI, diffusion-weighted imaging and (1)H-MR spectroscopy compared with histology (subgroup in the RAXO trial). *ESMO Open* 2021; **6**: 100208 [PMID: 34325107 DOI: 10.1016/j.esmoop.2021.100208]

23   **Harrison L**, Blackwell K. Hypoxia and anemia: factors in decreased sensitivity to radiation therapy and chemotherapy? *Oncologist* 2004; **9** Suppl 5: 31-40 [PMID: 15591420 DOI: 10.1634/theoncologist.9-90005-31]

24   **Xie JW**, Lu J, Xu BB, Zheng CH, Li P, Wang JB, Lin JX, Chen QY, Cao LL, Lin M, Tu RH, Huang ZN, Lin JL, Truty MJ, Huang CM. Prognostic Value of Tumor Regression Grading in Patients Treated With Neoadjuvant Chemotherapy Plus Surgery for Gastric Cancer. *Front Oncol* 2021; **11**: 587856 [PMID: 34386413 DOI: 10.3389/fonc.2021.587856]

25   **Tong Y**, Zhu Y, Zhao Y, Shan Z, Zhang J, Liu D. Tumor Regression Grade Predicts Survival in Locally Advanced Gastric Adenocarcinoma Patients with Lymph Node Metastasis. *Gastroenterol Res Pract* 2020; **2020**: 3435673 [PMID: 32733550 DOI: 10.1155/2020/3435673]

26   **Kim JH**, Joo I, Kim TY, Han SW, Kim YJ, Lee JM, Han JK. Diffusion-Related MRI Parameters for Assessing Early Treatment Response of Liver Metastases to Cytotoxic Therapy in Colorectal Cancer. *AJR Am J Roentgenol* 2016; **207**: W26-W32 [PMID: 27303858 DOI: 10.2214/AJR.15.15683]

27   **Jensen JH**, Helpern JA, Ramani A, Lu H, Kaczynski K. Diffusional kurtosis imaging: the quantification of non-gaussian water diffusion by means of magnetic resonance imaging. *Magn Reson Med* 2005; **53**: 1432-1440 [PMID: 15906300 DOI: 10.1002/mrm.20508]

28   **Zhou Y**, Zhang HX, Zhang XS, Sun YF, He KB, Sang XQ, Zhu YM, Kuai ZX. Non-mono-exponential diffusion models for assessing early response of liver metastases to chemotherapy in colorectal Cancer. *Cancer Imaging* 2019; **19**: 39 [PMID: 31217036 DOI: 10.1186/s40644-019-0228-2]

29   **Zhang H**, Li W, Fu C, Grimm R, Chen Z, Zhang W, Qiu L, Wang C, Zhang X, Yue L, Hu X, Guo W, Tong T. Comparison of intravoxel incoherent motion imaging, diffusion kurtosis imaging, and conventional DWI in predicting the chemotherapeutic response of colorectal liver metastases. *Eur J Radiol* 2020; **130**: 109149 [PMID: 32659615 DOI: 10.1016/j.ejrad.2020.109149]

30   **Chiaradia M**, Baranes L, Van Nhieu JT, Vignaud A, Laurent A, Decaens T, Charles-Nelson A, Brugières P, Katsahian S, Djabbari M, Deux JF, Sobhani I, Karoui M, Rahmouni A, Luciani A. Intravoxel incoherent motion (IVIM) MR imaging of colorectal liver metastases: are we only looking at tumor necrosis? *J Magn Reson Imaging* 2014; **39**: 317-325 [PMID: 23723012 DOI: 10.1002/jmri.24172]

31   **ter Voert EG**, Heijmen L, van Laarhoven HW, Heerschap A. In vivo magnetic resonance spectroscopy of liver tumors and metastases. *World J Gastroenterol* 2011; **17**: 5133-5149 [PMID: 22215937 DOI: 10.3748/wjg.v17.i47.5133]

32   **Ljungberg M**, Westberg G, Vikhoff-Baaz B, Starck G, Wängberg B, Ekholm S, Ahlman H, Forssell-Aronsson E. 31P MR spectroscopy to evaluate the efficacy of hepatic artery embolization in the treatment of neuroendocrine liver metastases. *Acta Radiol* 2012; **53**: 1118-1126 [PMID: 23051638 DOI: 10.1258/ar.2012.120050]

33   **Kamm YJ**, Heerschap A, van den Bergh EJ, Wagener DJ. 19F-magnetic resonance spectroscopy in patients with liver metastases of colorectal cancer treated with 5-fluorouracil. *Anticancer Drugs* 2004; **15**: 229-233 [PMID: 15014355 DOI: 10.1097/00001813-200403000-00006]

34   **Hahn OM**, Yang C, Medved M, Karczmar G, Kistner E, Karrison T, Manchen E, Mitchell M, Ratain MJ, Stadler WM. Dynamic contrast-enhanced magnetic resonance imaging pharmacodynamic biomarker study of sorafenib in metastatic renal carcinoma. *J Clin Oncol* 2008; **26**: 4572-4578 [PMID: 18824708 DOI: 10.1200/JCO.2007.15.5655]

35   **Saito K**, Ledsam J, Sugimoto K, Sourbron S, Araki Y, Tokuuye K. DCE-MRI for Early Prediction of Response in Hepatocellular Carcinoma after TACE and Sorafenib Therapy: A Pilot Study. *J Belg Soc Radiol* 2018; **102**: 40 [PMID: 30039052 DOI: 10.5334/jbsr.1278]

36   **Guo W**, Zhang Y, Luo D, Yuan H. Dynamic contrast-enhanced magnetic resonance imaging (DCE-MRI) for pretreatment prediction of neoadjuvant chemotherapy response in locally advanced hypopharyngeal cancer. *Br J Radiol* 2020; **93**: 20200751 [PMID: 32915647 DOI: 10.1259/bjr.20200751]

37   **Coenegrachts K**, Bols A, Haspeslagh M, Rigauts H. Prediction and monitoring of treatment effect using T1-weighted dynamic contrast-enhanced magnetic resonance imaging in colorectal liver metastases: potential of whole tumour ROI and selective ROI analysis. *Eur J Radiol* 2012; **81**: 3870-3876 [PMID: 22944331 DOI: 10.1016/j.ejrad.2012.07.022]

38   **Hirashima Y**, Yamada Y, Tateishi U, Kato K, Miyake M, Horita Y, Akiyoshi K, Takashima A, Okita N, Takahari D, Nakajima T, Hamaguchi T, Shimada Y, Shirao K. Pharmacokinetic parameters from 3-Tesla DCE-MRI as surrogate biomarkers of antitumor effects of bevacizumab plus FOLFIRI in colorectal cancer with liver metastasis. *Int J Cancer* 2012; **130**: 2359-2365 [PMID: 21780098 DOI: 10.1002/ijc.26282]

39   **Kim YE**, Joo B, Park MS, Shin SJ, Ahn JB, Kim MJ. Dynamic Contrast-Enhanced Magnetic Resonance Imaging as a Surrogate Biomarker for Bevacizumab in Colorectal Cancer Liver Metastasis: A Single-Arm, Exploratory Trial. *Cancer Res Treat* 2016; **48**: 1210-1221 [PMID: 26987390 DOI: 10.4143/crt.2015.374]

40   **De Bruyne S**, Van Damme N, Smeets P, Ferdinande L, Ceelen W, Mertens J, Van de Wiele C, Troisi R, Libbrecht L, Laurent S, Geboes K, Peeters M. Value of DCE-MRI and FDG-PET/CT in the prediction of response to preoperative chemotherapy with bevacizumab for colorectal liver metastases. *Br J Cancer* 2012; **106**: 1926-1933 [PMID: 22596235 DOI: 10.1038/bjc.2012.184]

41   **O'Connor JP**, Tofts PS, Miles KA, Parkes LM, Thompson G, Jackson A. Dynamic contrast-enhanced imaging techniques: CT and MRI. *Br J Radiol* 2011; **84** Spec No 2: S112-S120 [PMID: 22433822 DOI: 10.1259/bjr/55166688]

42   **Murata S**, Matsushima S, Sato Y, Yamaura H, Kato M, Hasegawa T, Muro K, Inaba Y. Predicting chemotherapeutic response for colorectal liver metastases using relative tumor enhancement of gadoxetic acid disodium-enhanced magnetic resonance imaging. *Abdom Radiol (NY)* 2018; **43**: 3301-3306 [PMID: 29666951 DOI: 10.1007/s00261-018-1615-z]

43   **Miles KA**, Leggett DA, Kelley BB, Hayball MP, Sinnatamby R, Bunce I. In vivo assessment of neovascularization of liver metastases using perfusion CT. *Br J Radiol* 1998; **71**: 276-281 [PMID: 9616236 DOI: 10.1259/bjr.71.843.9616236]

44   **Joo I**, Lee JM, Kim KW, Klotz E, Han JK, Choi BI. Liver metastases on quantitative color mapping of the arterial enhancement fraction from multiphasic CT scans: evaluation of the hemodynamic features and correlation with the chemotherapy response. *Eur J Radiol* 2011; **80**: e278-e283 [PMID: 21251785 DOI: 10.1016/j.ejrad.2010.12.002]

45   **Kim DH**, Kim SH, Im SA, Han SW, Goo JM, Willmann JK, Lee ES, Eo JS, Paeng JC, Han JK, Choi BI. Intermodality comparison between 3D perfusion CT and 18F-FDG PET/CT imaging for predicting early tumor response in patients with liver metastasis after chemotherapy: preliminary results of a prospective study. *Eur J Radiol* 2012; **81**: 3542-3550 [PMID: 22459347 DOI: 10.1016/j.ejrad.2012.02.012]

46   **Osawa G**, Yoshimatsu K, Yokomizo H, Okayama S, Sagawa M, Naritaka Y. Correlation between response to chemotherapy with concomitant bevacizumab for hepatic metastasis of colorectal cancer and degree of enhancement using contrast-enhanced computed tomography. *Cancer Chemother Pharmacol* 2013; **72**: 209-215 [PMID: 23670642 DOI: 10.1007/s00280-013-2186-x]

47   **Mainenti PP**, Salvatore B, D'Antonio D, De Falco T, De Palma GD, D'Armiento FP, Bucci L, Pace L, Salvatore M. PET/CT colonography in patients with colorectal polyps: a feasibility study. *Eur J Nucl Med Mol Imaging* 2007; **34**: 1594-1603 [PMID: 17492447 DOI: 10.1007/s00259-007-0422-5]

48   **Mainenti PP**, Stanzione A, Guarino S, Romeo V, Ugga L, Romano F, Storto G, Maurea S, Brunetti A. Colorectal cancer: Parametric evaluation of morphological, functional and molecular tomographic imaging. *World J Gastroenterol* 2019; **25**: 5233-5256 [PMID: 31558870 DOI: 10.3748/wjg.v25.i35.5233]

49   **Kocael A**, Vatankulu B, Şimşek O, Cengiz M, Kemik A, Kocael P, Halaç M, Sönmezoğlu K, Ulualp K. Comparison of (18)F-fluorodeoxyglucose PET/CT findings with vascular endothelial growth factors and receptors in colorectal cancer. *Tumour Biol* 2016; **37**: 3871-3877 [PMID: 26476536 DOI: 10.1007/s13277-015-4218-0]

50   **Byström P**, Berglund A, Garske U, Jacobsson H, Sundin A, Nygren P, Frödin JE, Glimelius B. Early prediction of response to first-line chemotherapy by sequential [18F]-2-fluoro-2-deoxy-D-glucose positron emission tomography in patients with advanced colorectal cancer. *Ann Oncol* 2009; **20**: 1057-1061 [PMID: 19164458 DOI: 10.1093/annonc/mdn744]

51   **Hendlisz A**, Golfinopoulos V, Garcia C, Covas A, Emonts P, Ameye L, Paesmans M, Deleporte A, Machiels G, Toussaint E, Vanderlinden B, Awada A, Piccart M, Flamen P. Serial FDG-PET/CT for early outcome prediction in patients with metastatic colorectal cancer undergoing chemotherapy. *Ann Oncol* 2012; **23**: 1687-1693 [PMID: 22112970 DOI: 10.1093/annonc/mdr554]

52   **Mertens J**, De Bruyne S, Van Damme N, Smeets P, Ceelen W, Troisi R, Laurent S, Geboes K, Peeters M, Goethals I, Van de Wiele C. Standardized added metabolic activity (SAM) IN ¹⁸F-FDG PET assessment of treatment response in colorectal liver metastases. *Eur J Nucl Med Mol Imaging* 2013; **40**: 1214-1222 [PMID: 23636802 DOI: 10.1007/s00259-013-2421-z]

53   **Mertens J**, Dobbeleir A, Ham H, D'Asseler Y, Goethals I, Van de Wiele C. Standardized added metabolic activity (SAM): a partial volume independent marker of total lesion glycolysis in liver metastases. *Eur J Nucl Med Mol Imaging* 2012; **39**: 1441-1448 [PMID: 22699529 DOI: 10.1007/s00259-012-2166-0]

54   **Heijmen L**, ter Voert EE, Oyen WJ, Punt CJ, van Spronsen DJ, Heerschap A, de Geus-Oei LF, van Laarhoven HW. Multimodality imaging to predict response to systemic treatment in patients with advanced colorectal cancer. *PLoS One* 2015; **10**: e0120823 [PMID: 25831053 DOI: 10.1371/journal.pone.0120823]

55   **Rogers W**, Thulasi Seetha S, Refaee TAG, Lieverse RIY, Granzier RWY, Ibrahim A, Keek SA, Sanduleanu S, Primakov SP, Beuque MPL, Marcus D, van der Wiel AMA, Zerka F, Oberije CJG, van Timmeren JE, Woodruff HC, Lambin P. Radiomics: from qualitative to quantitative imaging. *Br J Radiol* 2020; **93**: 20190948 [PMID: 32101448 DOI: 10.1259/bjr.20190948]

56   **Cuocolo R**, Caruso M, Perillo T, Ugga L, Petretta M. Machine Learning in oncology: A clinical appraisal. *Cancer Lett* 2020; **481**: 55-62 [PMID: 32251707 DOI: 10.1016/j.canlet.2020.03.032]

57   **Alves AFF**, Miranda JRA, Reis F, de Souza SAS, Alves LLR, Feitoza LM, de Castro JTS, de Pina DR. Inflammatory lesions and brain tumors: is it possible to differentiate them based on texture features in magnetic resonance imaging? *J Venom Anim Toxins Incl Trop Dis* 2020; **26**: e20200011 [PMID: 32952531 DOI: 10.1590/1678-9199-JVATITD-2020-0011]

58   **Kassner A**, Thornhill RE. Texture analysis: a review of neurologic MR imaging applications. *AJNR Am J Neuroradiol* 2010; **31**: 809-816 [PMID: 20395383 DOI: 10.3174/ajnr.A2061]

59   **Ahn SJ**, Kim JH, Park SJ, Han JK. Prediction of the therapeutic response after FOLFOX and FOLFIRI treatment for patients with liver metastasis from colorectal cancer using computerized CT texture analysis. *Eur J Radiol* 2016; **85**: 1867-1874 [PMID: 27666629 DOI: 10.1016/j.ejrad.2016.08.014]

60   **Ravanelli M**, Agazzi GM, Tononcelli E, Roca E, Cabassa P, Baiocchi G, Berruti A, Maroldi R, Farina D. Texture features of colorectal liver metastases on pretreatment contrast-enhanced CT may predict response and prognosis in patients treated with bevacizumab-containing chemotherapy: a pilot study including comparison with standard chemotherapy. *Radiol Med* 2019; **124**: 877-886 [PMID: 31172448 DOI: 10.1007/s11547-019-01046-4]

61   **Creasy JM**, Midya A, Chakraborty J, Adams LB, Gomes C, Gonen M, Seastedt KP, Sutton EJ, Cercek A, Kemeny NE, Shia J, Balachandran VP, Kingham TP, Allen PJ, DeMatteo RP, Jarnagin WR, D'Angelica MI, Do RKG, Simpson AL. Quantitative imaging features of pretreatment CT predict volumetric response to chemotherapy in patients with colorectal liver metastases. *Eur Radiol* 2019; **29**: 458-467 [PMID: 29922934 DOI: 10.1007/s00330-018-5542-8]

62   **Liang HY**, Huang YQ, Yang ZX, Ying-Ding, Zeng MS, Rao SX. Potential of MR histogram analyses for prediction of response to chemotherapy in patients with colorectal hepatic metastases. *Eur Radiol* 2016; **26**: 2009-2018 [PMID: 26494642 DOI: 10.1007/s00330-015-4043-2]

63   **Zhang H**, Li W, Hu F, Sun Y, Hu T, Tong T. MR texture analysis: potential imaging biomarker for predicting the chemotherapeutic response of patients with colorectal liver metastases. *Abdom Radiol (NY)* 2019; **44**: 65-71 [PMID: 29967982 DOI: 10.1007/s00261-018-1682-1]

64   **Rabe E**, Cioni D, Baglietto L, Fornili M, Gabelloni M, Neri E. Can the computed tomography texture analysis of colorectal liver metastases predict the response to first-line cytotoxic chemotherapy? *World J Hepatol* 2022; **14**: 244-259 [PMID: 35126852 DOI: 10.4254/wjh.v14.i1.244]

65   **Giannini V**, Defeudis A, Rosati S, Cappello G, Mazzetti S, Panic J, Regge D, Balestra G. An innovative radiomics approach to predict response to chemotherapy of liver metastases based on CT images. *Annu Int Conf IEEE Eng Med Biol Soc* 2020; **2020**: 1339-1342 [PMID: 33018236 DOI: 10.1109/EMBC44109.2020.9176627]

66   **Giannini V**, Rosati S, Defeudis A, Balestra G, Vassallo L, Cappello G, Mazzetti S, De Mattia C, Rizzetto F, Torresin A, Sartore-Bianchi A, Siena S, Vanzulli A, Leone F, Zagonel V, Marsoni S, Regge D. Radiomics predicts response of individual HER2-amplified colorectal cancer liver metastases in patients treated with HER2-targeted therapy. *Int J Cancer* 2020; **147**: 3215-3223 [PMID: 32875550 DOI: 10.1002/ijc.33271]

67   **Siravegna G**, Lazzari L, Crisafulli G, Sartore-Bianchi A, Mussolin B, Cassingena A, Martino C, Lanman RB, Nagy RJ, Fairclough S, Rospo G, Corti G, Bartolini A, Arcella P, Montone M, Lodi F, Lorenzato A, Vanzati A, Valtorta E, Cappello G, Bertotti A, Lonardi S, Zagonel V, Leone F, Russo M, Balsamo A, Truini M, Di Nicolantonio F, Amatu A, Bonazzina E, Ghezzi S, Regge D, Vanzulli A, Trusolino L, Siena S, Marsoni S, Bardelli A. Radiologic and Genomic Evolution of Individual Metastases during HER2 Blockade in Colorectal Cancer. *Cancer Cell* 2018; **34**: 148-162.e7 [PMID: 29990497 DOI: 10.1016/j.ccell.2018.06.004]

68   **Wei J**, Cheng J, Gu D, Chai F, Hong N, Wang Y, Tian J. Deep learning-based radiomics predicts response to chemotherapy in colorectal liver metastases. *Med Phys* 2021; **48**: 513-522 [PMID: 33119899 DOI: 10.1002/mp.14563]